33rd European Modeling & Simulation Symposium
18th International Multidisciplinary Modeling & Simulation Multiconference

ISSN 2724-0029 ISBN 978-88-85741-57-7 © 2021 The Authors.
doi: 10.46354/i3m.2021.emss.047

Estimation of optimal positioning of gold contact pads for modulating nanophotonic devices based on lithium niobate on insulator platform

Ilia Elmanov[1*], Anna Elmanova[1], Vadim Kovalyuk[1], Pavel An[1] and Gregory Goltsman[1,2]

[1]Department of Physics, Moscow Pedagogical State University (MPGU), 119992, Russia
[2]National Research University Higher School of Economics, Moscow 101000, Russia
*Email address: ilia22870@gmail.com

Abstract

Using a numerical simulation of a cross-section of lithium niobate (LN) waveguide, we have determined the optimal position of gold contact pads near the waveguide to better utilize the electro-optic effect in lithium niobate. Varying such parameters as contact thickness, the distance between them, thickness of additional silicon oxide covering, and thickness of remaining not etched LN layer, we determined the value of optical absorption in such configuration and electric field value near to the sidewall of the waveguide. As a result, we determined an optimal configuration, which corresponds to the maximum electric field with a satisfactory value of optical losses.

Keywords: photonic integrated circuit, lithium niobate on insulator; electro-optical modulator

1. Introduction

Lithium niobate is a widely used material that in the optical industry due to its exceptional properties. From them, we may highlight a high refractive index, wide transparency window (Zelmon, Small and Jundt. 1997), and exceptional electro-optical properties (Lenzo, Spencer, and Nassau, 1966). This materials electro-optical properties apply in electro-optical high-frequency modulators (EOM) (Binh, 2006). Like the development of such devices in bulk LN, researchers create of EOM based on integrated photonics technologies (Wang et al., 2018). On-chip integrated photonics allows us to produce different optical devices in much lower scales and make them easily scalable and rather cheap. Also, such realization of LN based EOMs will allow obtaining higher efficiency concerning to the bulk one. Furthermore, development of such modulators is necessary for the development of on-chip quantum photonics devices (Moody et al., 2021), because such EOMs can operate at cryogenic temperatures. In the majority of modern researches, such modulators realized as a Mach-Zehnder interferometers, where manipulation of optical path length in arms realized throw applying an external electric field around the waveguide, and due to the electro-optical effect in LN, this field introduces some change in the refractive index of the material in each arm. This change provides a phase difference between arms leading to different interference fringes. The change of optical path will depend on the value of the external electric field near the waveguide (Wang et al., 2018). Of course, the electric field will be higher if we place contacts closer to each other. Still, metal near the optical waveguide will lead to additional losses of optical radiation. But some configurations of our device may have a higher electric field with lower losses concerning other ones. In this work, we study how different geometry parameters of our device will influence the values of optical absorption and electric field.

2. Materials and Methods

For our study, we chose a simple design with symmetric gold contacts near to walls of the strip waveguide on the silica layer. Such a scheme was chosen to produce an electric field perpendicular to the waveguide and directed along the z-axis of the LN crystal. It is also possible to sputter an additional silicon oxide layer on our sample for its protection, isolation of gold contacts, or the possibility of placing our contacts higher. Because of features of the process of ion etching of LN waveguides are usually have some sidewall inclination angle (Siew et al., 2018). Our model considered this fact and includes the sidewall inclination equals 60 degrees. We have used the finite elements method (FEM) to calculate the optical losses and values of the electric field (E-field), realized in COMSOL Multiphysics software. In our simulation we varied the thickness of contacts (h_{cont}), the distance between the edge of waveguide and contact pad (*gap*), the thickness of additional silicon oxide sputtering (*cover*) and the thickness of residual LN layer, because it is not always possible to etch LN film on the full depth.

3. Modeling

We used a cross-section model of strip LN waveguide placed over the silicon oxide layer (Figure 1). The thickness of LN was chosen as 600 nm due to our access to such wafers for further fabrication. In the simulation, thicknesses of an insulating layer of silicon oxide and air were determined as enough for separating of our waveguide and contacts from the borders of the model. Sidewall angle inclination was set as 60 degrees because this value is close to the experimental results. The width of the lower part of waveguide was 1 μm for single-mode propagation of optical radiation at wavelength 1550 nm.

Using this simulation, we started to change parameters influencing on electric field and optical absorption. We took some finite number of parameters, and changed h_{cont} in range from 125 nm to 500 nm (limited by fabrication process) with step 125 nm; silicon oxide *cover* in the range from 100 nm to 1000 nm with step 100 nm; *gap* in the range 250 nm to 2000 nm with step 250 nm and thickness of residual LN layer from 10 nm to 90 nm with step 20 nm. After a fully etched LN case, the simulation of the presence of residual layer of LN was done without additional silicon oxide cover. Obtained data transferred to the table format for further analysis. Value of optical losses was found by COMSOL Multiphysics. Electric field value was taken as an average value of x-component of electric field along the line close and parallel to the sidewall of our waveguide. We have plotted the electric field vs absorption graph to find points that may have a high electric field value with relatively low optical losses. Also we tried to keep our losses lower than 10 dB/m (Figure 2). After that, we looked at exact values at these points and got values of varying parameters (Table 1 and Table 2).

4. Results and Discussion

In general, we obtained predictable results, where electric field and absorption increased simultaneously. However, we found some points with a higher field with lower losses than their neighbors or a much higher field with a small increase in attenuation (marked in red in Figure 2). Such points have parameters h_{cont} = 500 nm, *gap* = 750 nm, *cover* = 100 nm, which lead to electric field equals to 4.1 MV/m and attenuation equals to 4.32 dB/m for simulation with fully etched LN layer and h_{cont} = 500 nm, *gap* = 750 nm, residual thickness of LN = 10 nm which lead to electric field equals to 4.73 MV/m and attenuation equals to 4.93 dB/m for simulation with not fully etched LN. Our results are limited by the steps of parameters changing and not simulated additional covering for the model with some not etched LN. Still the simulated points for model with a residual layer of LN shows the best performance. Also, as it can be seen from Table 1 majority of good results have a gap parameter equals to 750 nm. Fixing the gap at this value, we have plotted dependences of E-field and attenuation from contact thickness and silicon oxide additional layer (Figure 3 a, b). With fixed gap increase of silicon oxide layer will lead to decrease in attenuation due to further isolation of contact pads from waveguide. After the same reason electric field will also will descend. These graphs show that it is useful to use thicker contact pads simultaneously with thinner silicon oxide cover. For the model with the residual LN layer, we have fixed thickness of this residual layer at 10 nm, and plotted color maps for attenuation (Figure 4, a) and E-field (Figure 4, b) with variables of gap and contact pads thickness. For both cases increasing of pads thickness will lead to higher values of E-field, together with more uniform E-field distribution.

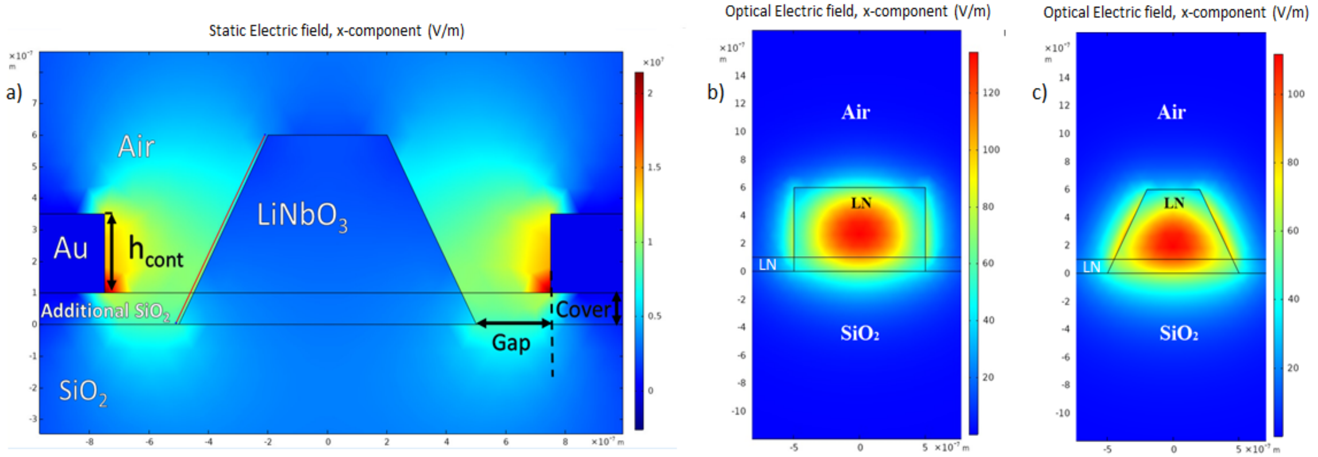

Figure 1. a) Numerical simulation of electric field distribution of static electric field from contact pads for waveguide cross-section with gold pads on each side. The red line on the left side of the waveguide's wall is a line along which we calculated the average value of the electric field. **b)** Optical electric field distribution for rectangular shape of waveguide. **c)** Optical electric field distribution for waveguide with sidewall inclination.

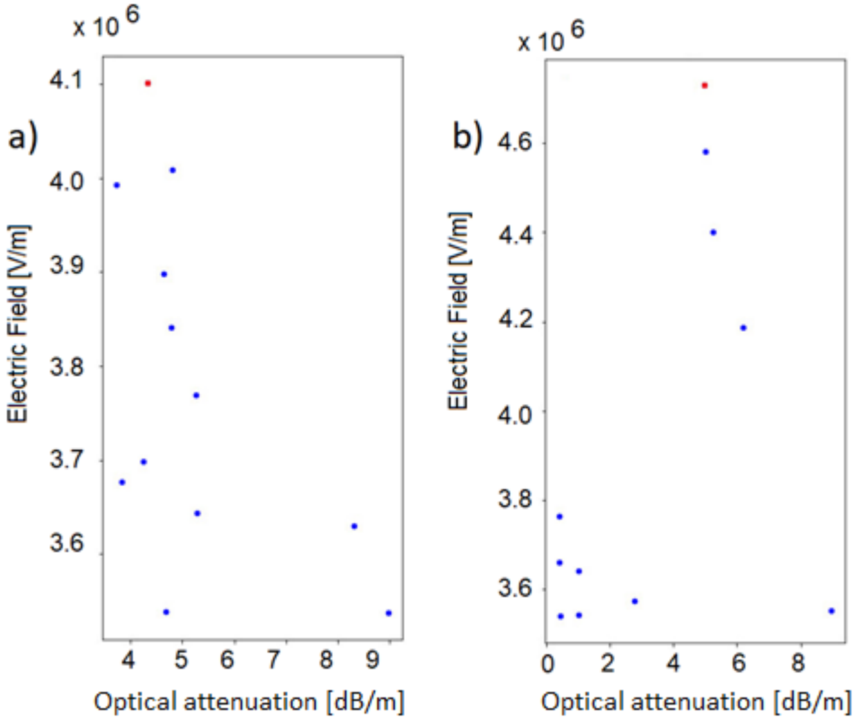

Figure 2. Set of points with highest electric field under the condition of attenuation lower than 10 dB/m for simulation without residual layer of LN (a) and with such layer (b)

Table 1. Parameters for points from figure 2 (a)

h_cont (nm)	gap (nm)	cover (μm)	Attenuation (dB/m)	E field (V/m)
250	750	0	3.835406	3.676790*10^6
500	750	0	3.717270	3.993441*10^6
250	500	0.9	8.990746	3.537709*10^6
500	500	0.9	8.316266	3.630222*10^6
250	750	0.1	4.630984	3.898442*10^6
250	750	0.2	5.254567	3.769900*10^6
250	750	0.3	5.285711	3.644180*10^6
250	750	0.4	4.671956	3.538498*10^6
500	750	0.1	4.321000	4.101341*10^6
500	750	0.2	4.801269	4.009291*10^6
500	750	0.3	4.792137	3.841287*10^6
500	750	0.4	4.233211	3.699169*10^6

Table 2. Parameters for points from figure 2 (b)

h_cont (nm)	gap (nm)	Residual layer of	Attenuation (dB/m)	E field (V/m)

		LN (nm)		
125	750	10	6.174988	4.186730*10^6
250	750	10	5.228785	4.399872*10^6
375	750	10	5.013894	4.580328*10^6
500	750	10	4.932630	4.728242*10^6
250	1000	10	0.431409	3.539762*10^6
375	1000	10	0.410998	3.660583*10^6
375	1000	30	1.027332	3.541959*10^6
500	1000	10	0.402634	3.764185*10^6
500	1000	30	1.003013	3.640147*10^6
500	1000	50	2.777093	3.574764*10^6
500	1000	70	8.972606	3.551193*10^6
125	750	10	6.174988	4.186730*10^6

5. Conclusions

In this paper, we studied the dependence of electric field and optical losses from the positioning of gold contacts along the waveguide. The highest E-field value, equals 4.7 MV/m, was achieved with attenuation equals 4.93 dB/m. It was shown that for better performance it is useful to make contact pads thicker and place them at a distance close to 750 nm from the waveguide. Also, it will be better to use a thin silicon oxide layer if LN will be fully etched. Our results may be helpful for the development and fabrication of optical integrated reconfigurable devices based on the LNOI platform, providing the possibility to increase their efficiency. However, our results are limited by the fact of rather huge steps in sweeping parameters, and absence of simulation for the model with residual LN layer together with an additional silicon oxide layer, but it should be enough for estimation of main parameters with satisfactory accuracy.

Funding

The research was performed by support of the Russian Science Foundation grant No. 19-72-10156.

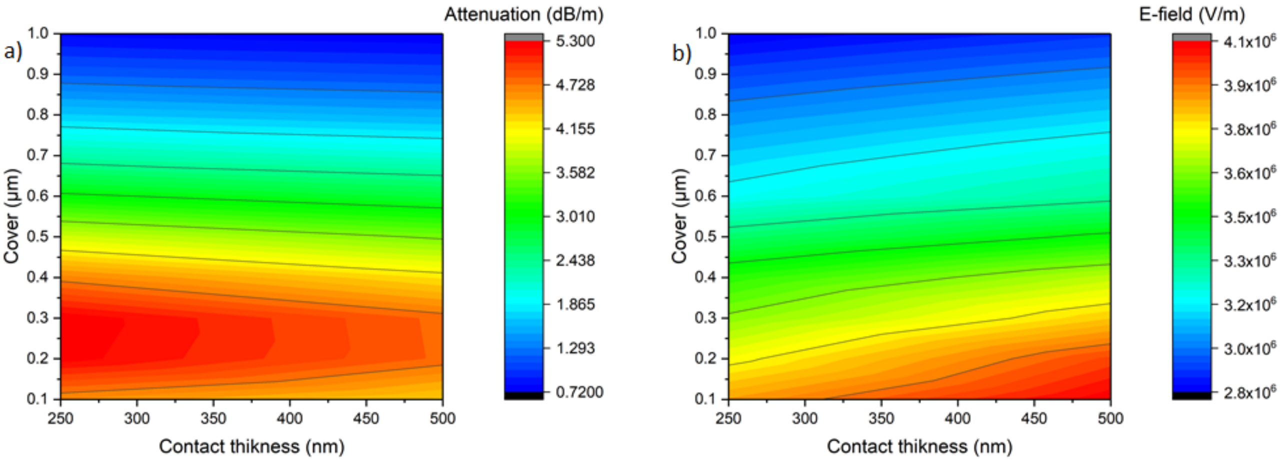

Figure 3. Attenuation (a) and E-field (b) vs cover and contact thickness for model with additional silicon cover with fixed gap equals 750 nm.

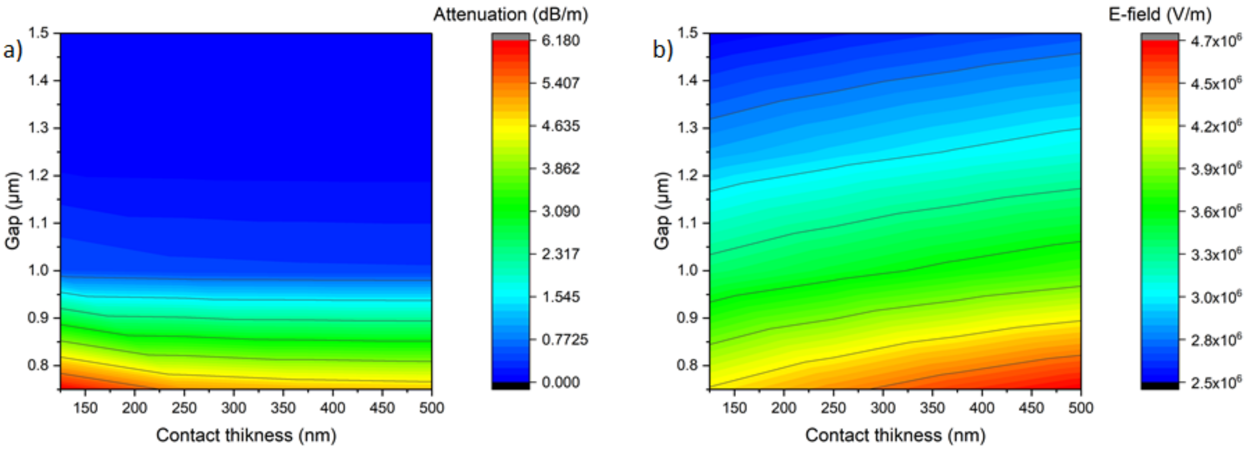

Figure 4. Attenuation (a) and E-field (b) vs gap and contact thickness for the model with residual LN layer with fixed residual LN layer thickness equals 10 nm.

References

Binh L. N. (2006) Lithium niobate optical modulators: Devices and applications, *Journal of Crystal Growth*, Volume 288, Issue 1, 180-187

Lenzo P. V., Spencer E. G., and Nassau K. (1966) Electro-Optic Coefficients in Single-Domain Ferroelectric Lithium Niobate, *J. Opt. Soc. Am.* 56, 633-635

Moody G, et. al (2021) Roadmap on Integrated Quantum Photonics *arxiv.org*

Siew S. Y., et. al. (2018) Ultra-low loss ridge waveguides on lithium niobate via argon ion milling and gas clustered ion beam smoothening, *Opt. Express* 26, 4421-4430

Wang C., Zhang M., Stern B., Lipson M., and Lončar M. (2018) Nanophotonic lithium niobate electro-optic modulators, *Opt. Express* 26, 1547-1555

Zelmon D. E., Small D. L., and Jundt D. (1997) Infrared corrected Sellmeier coefficients for congruently grown lithium niobate and 5 mol.% magnesium oxide–doped lithium niobate, *J. Opt. Soc. Am.* B 14, 3319-3322